Measurements of $B \to V\gamma$ decays from BaBar

Kevin Yarritu
SLAC National Accelerator Laboratory

Fermi National
Accelerator Laboratory
October 13th, 2009

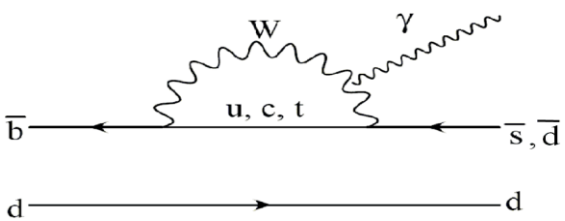

Outline of talk

1. Motivation to study $B \to V\gamma$ decays
2. The Babar detector
3. Measurement of Branching Fraction, CP, and Isospin Asymmetries in $B \to K^*\gamma$
4. Measurement of $B \to \rho(\omega)\gamma$ decays
5. Search for $B \to \varphi\gamma$
6. Conclusion

Motivation to study B $\rightarrow V\gamma$ decays

$b \to s(d)$ transitions

- Transition $B \to V\gamma$ ($V = K^*, \rho, \omega, \varphi$ in this talk) is a flavor changing neutral current.

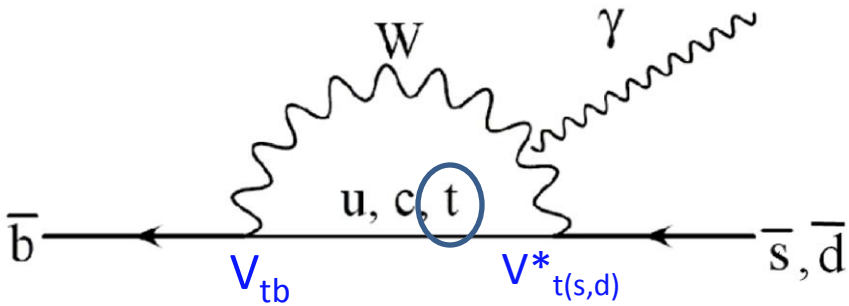

dominant diagram for $V = (K^*, \rho, \omega)$

- Top quark dominates in the loop
- Branching fraction of $B \to \rho\gamma$ is suppressed relative to $B \to K^*\gamma$ by a factor of $|V_{td}/V_{ts}|^2 \approx .04$.
- Magnitudes of the branching fractions are suppressed by $G_F^2 \alpha_{EM}$ ($\approx 10^{-5}$ ($B \to K^*\gamma$) and $\approx 10^{-6}$ ($B \to \rho/\omega\ \gamma$)).

New Physics

- Radiative decays are interesting because of the loop.
- Physics beyond the Standard Model could enter at the same order in perturbation theory as the Standard Model.

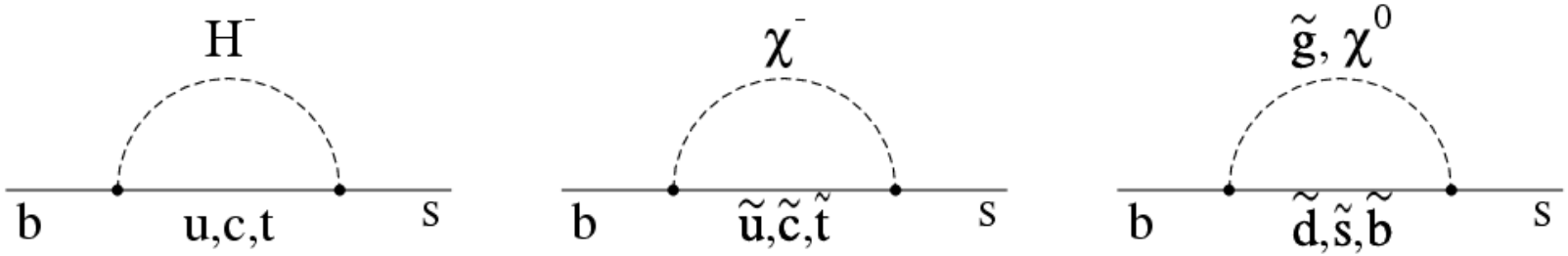

supersymmetric diagrams

- Choose observables, measure them, and then compare with the Standard Model values. If things are exciting, we will see deviations.

Hadronic Uncertainties

- Theoretical predictions for the branching fractions suffer from hadronic uncertainties

Prediction for B $\longrightarrow$ K*γ	Reference
$(5.8 \pm 2.9) \times 10^{-5}$ $(B^0 \to K^{*0}\gamma)$ $(6.0 \pm 3.0) \times 10^{-5}$ $(B^+ \to K^{*+}\gamma)$	Matsumori, Sanda, and Keum PRD 72 (2005) 014013
$(4.3 \pm 1.4) \times 10^{-5}$ $(B^0 \to K^{*0}\gamma)$ $(4.6 \pm 1.4) \times 10^{-5}$ $(B^+ \to K^{*+}\gamma)$	Ali, Pecjak, and Greub Eur. Phys. J.C55 (2008) 577

- Therefore, we choose different observables to look for new physics.

$B \to K^*\gamma$ CP asymmetry

The **CP** asymmetry is defined as:

$$\mathcal{A} = \frac{\Gamma(\overline{B} \to \overline{K}^*\gamma) - \Gamma(B \to K^*\gamma)}{\Gamma(\overline{B} \to \overline{K}^*\gamma) + \Gamma(B \to K^*\gamma)}$$

- Decay is dominated by a single Feynman diagram, and the CP asymmetry is $\approx \sin^6\theta_C$
- The unitarity triangle associated with $B \to K^*\gamma$

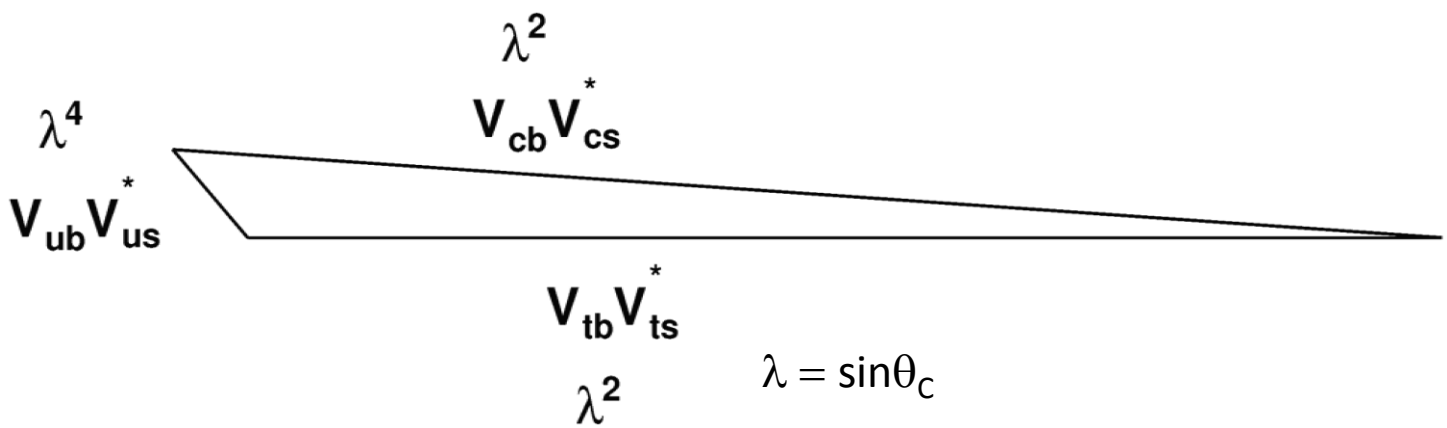

- $A_{CP} < 1\%$.

$B \to K^*\gamma$ isospin asymmetry

The **isospin** asymmetry (*u* and *d* difference) is defined as:

$$\Delta_{0+} \equiv \frac{\Gamma(B^0 \to K^{*0}\gamma) - \Gamma(B^+ \to K^{*+}\gamma)}{\Gamma(B^0 \to K^{*0}\gamma) + \Gamma(B^+ \to K^{*+}\gamma)}$$

($\Delta_{0+} = \Delta_{0-}$ with no CP violation)

- Leading contributions to the isospin asymmetry are

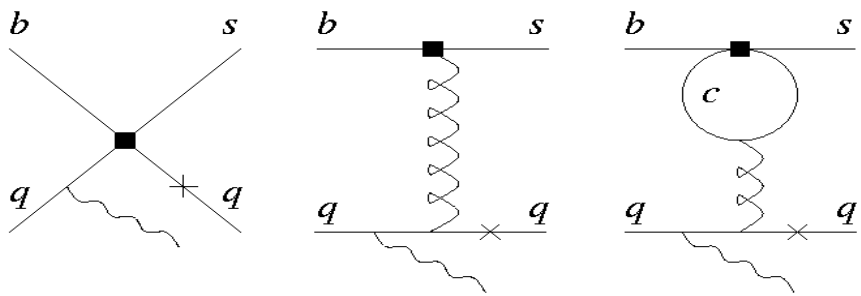

- Predictions that use the Standard Model are

$$\Delta_{0+} = +(2.6 \pm 0.8)\text{x } 10^{-2}\,, \quad \Delta_{0+} = +(8.0^{+2.1}_{-3.2})\text{x } 10^{-2}$$

Matsumori, Sanda, Keum
PRD 72, 014013 (2005)

Kagan and Neubert
Phys. Lett. B539 (2002)

Constraints on mSUGRA by isospin asymmetry

$-0.047 < \Delta_{0-} < 0.093$ (world average)

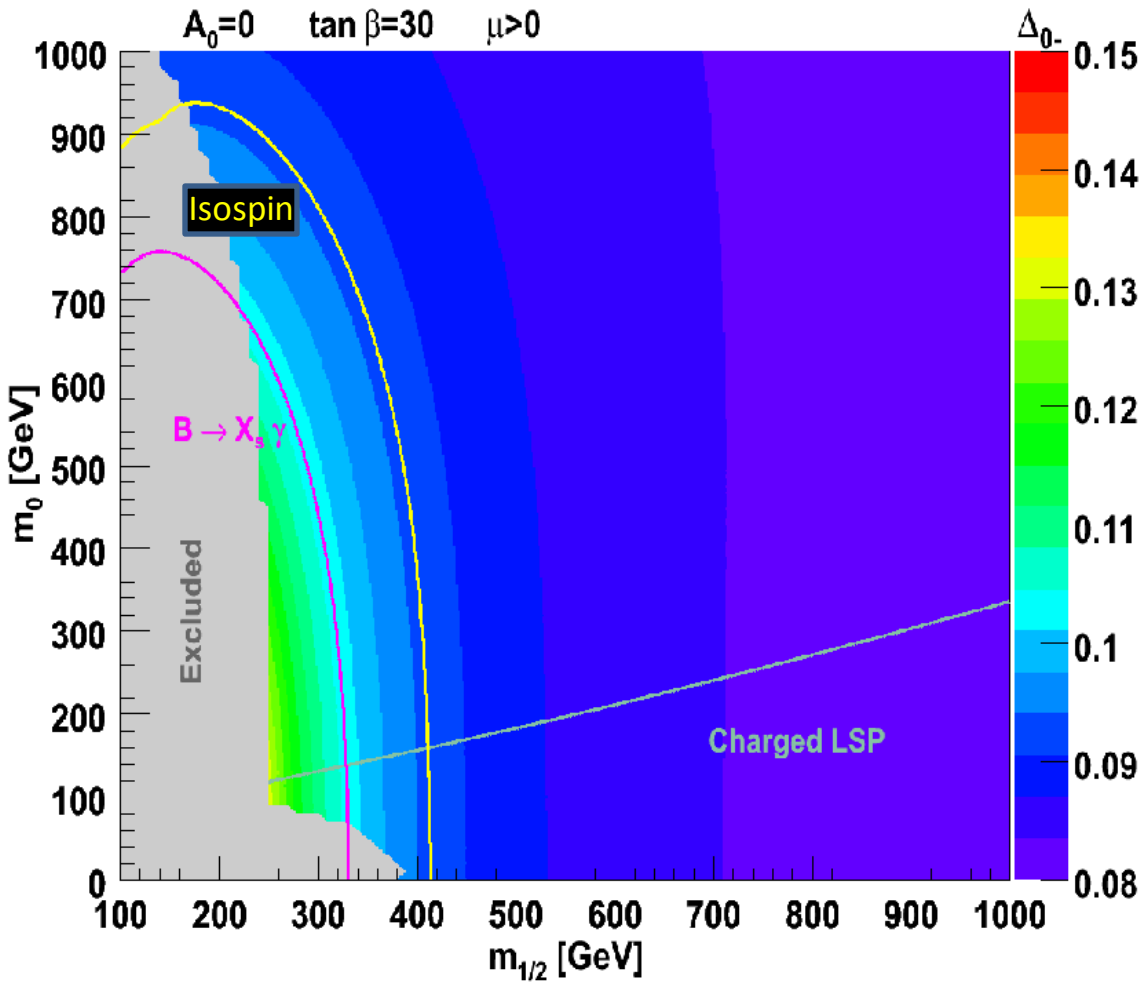

Ahmady and Mahmoudi hep-ph/0608212

$|V_{td}/V_{ts}|$

- The ratio $|V_{td}/V_{ts}|$ can be extracted by taking the ratio of $B \to \rho\gamma$ with $B \to K^*\gamma$.

- In the Wolfenstein parameterization, the CKM matrix is written as

$$V = \begin{pmatrix} V_{ud} & V_{us} & V_{ub} \\ V_{cd} & V_{cs} & V_{cb} \\ V_{td} & V_{ts} & V_{tb} \end{pmatrix} \Rightarrow V = \begin{pmatrix} 1-\frac{\lambda^2}{2} & \lambda & A\lambda^3(\rho - i\eta) \\ -\lambda & 1-\frac{\lambda^2}{2} & A\lambda^2 \\ A\lambda^3(1-\rho-i\eta) & -A\lambda^2 & 1 \end{pmatrix} + \mathcal{O}(\lambda^4)$$

where

$$\lambda = \frac{|V_{us}|}{\sqrt{|V_{ud}|^2 + |V_{us}|^2}} \qquad A\lambda = \left|\frac{V_{cb}}{V_{us}}\right| \qquad \bar{\rho} + i\bar{\eta} = -\frac{V_{ud}V_{ub}^*}{V_{cd}V_{cb}^*}$$

In the $\bar{\rho}$ - $\bar{\eta}$ plane, the canonical unitarity triangle is, when rescaled by $V^*_{cb}V_{cd}$

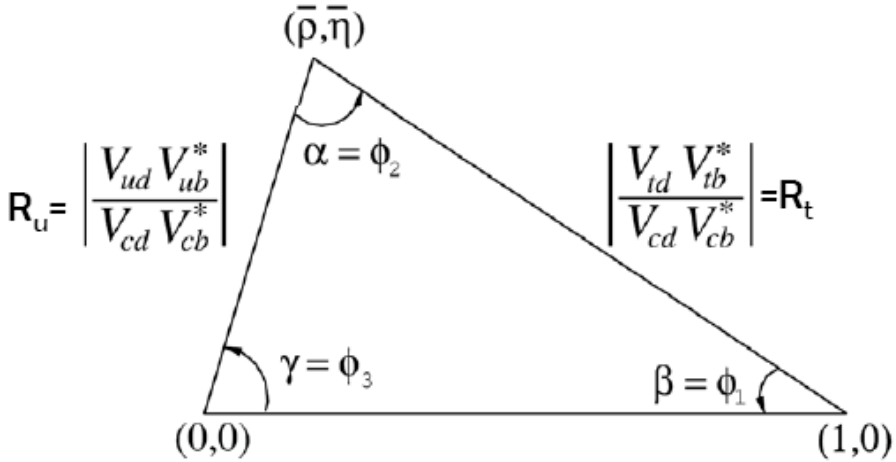

Using the Wolfenstein parameterization, R_t can rewritten as

$$R_t = \frac{1}{\lambda}\left|\frac{V_{td}}{V_{ts}}\right|$$

. Therefore, $|V_{td}/V_{ts}|$ corresponds to one side of the unitary triangle.

$|V_{td}/V_{ts}|$ extraction

$$\frac{\mathcal{B}[B \to (\rho/\omega)\gamma]}{\mathcal{B}[B \to K^*\gamma]} = \left|\frac{V_{td}}{V_{ts}}\right|^2 \left(\frac{1 - m_\rho^2/M_B^2}{1 - m_{K^*}^2/M_B^2}\right)^3 \zeta^2[1 + \Delta R]$$

where

$$\mathcal{B}(B \to (\rho,\omega)\gamma) = \frac{1}{2} \cdot \{\mathcal{B}(B^\pm \to \rho^\pm\gamma) + \frac{\tau_{B^+}}{\tau_{B^0}} \cdot [\mathcal{B}(B^0 \to \rho^0\gamma) + \mathcal{B}(B^0 \to \omega\gamma)]\}$$

ζ = 0.85 ± 0.07 is the ratio of form factors for the decays B $\longrightarrow$ $\rho\gamma$ and B $\longrightarrow$ K*γ (JHEP 04(2006)046)

ΔR = 0.1 ± 0.1 accounts for differences in dynamics of decays (e.g. annihilation diagrams) (PLB 595, 323 (2004))

Overview of the Babar detector

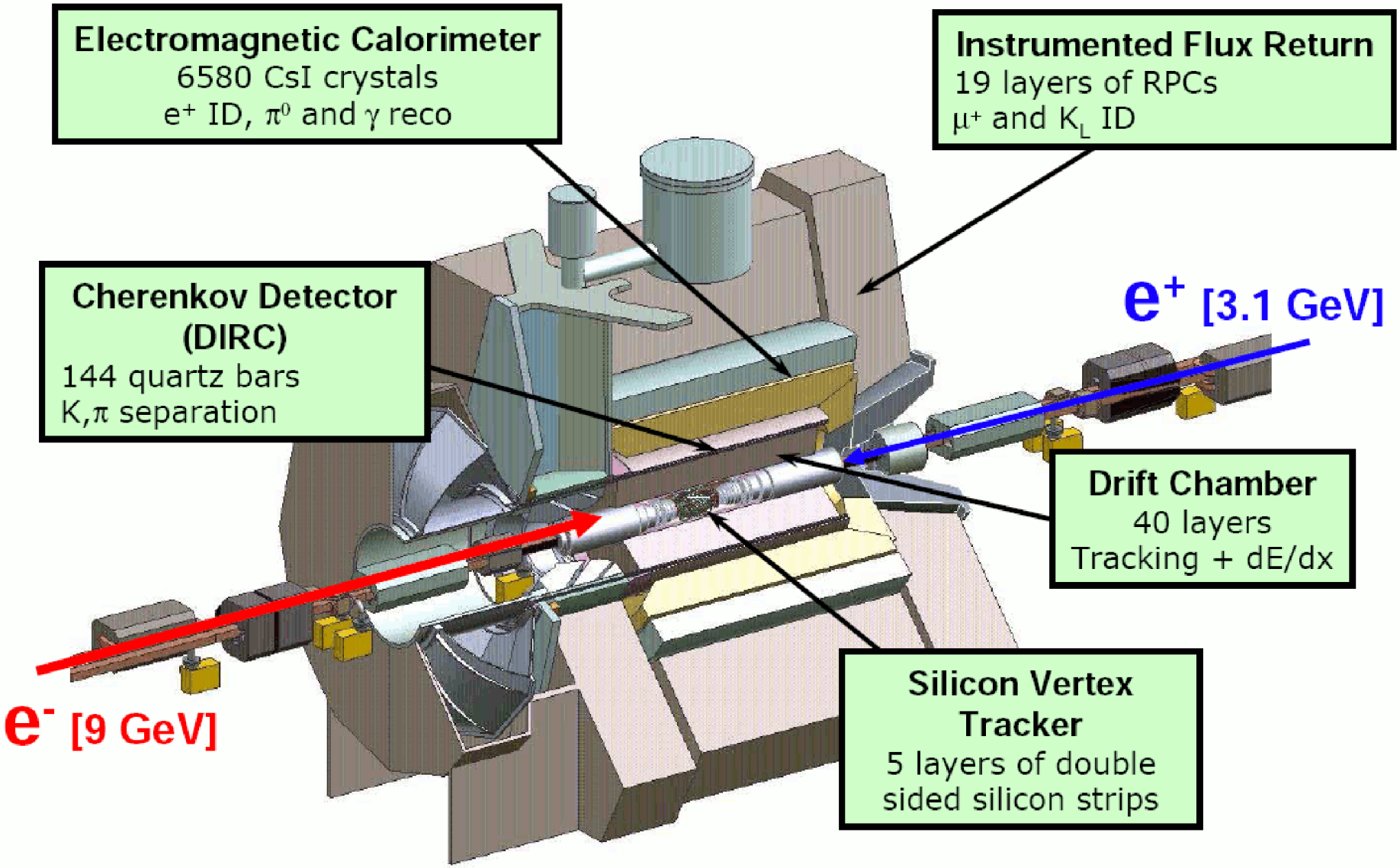
Electromagnetic Calorimeter
6580 CsI crystals
e+ ID, π0 and γ reco
Instrumented Flux Return
19 layers of RPCs
μ+ and KL ID
Cherenkov Detector (DIRC)
144 quartz bars
K,π separation
e+ [3.1 GeV]
Drift Chamber
40 layers
Tracking + dE/dx
e- [9 GeV]
Silicon Vertex Tracker
5 layers of double sided silicon strips

Particle Identification Overview

- Particle identification is required at Babar up to momentum of 4.2 GeV/c

- K/π separation is required for the momentum range 1.7 < $|p|$ < 4.2 GeV/c for rare charmless decays (e.g. B $\rightarrow \pi^+\pi^-$) and $p|$ < 2 GeV/c (e.g. B/$\bar{B}$ flavor identification by kaons via b $\rightarrow$ c $\rightarrow$ s)

- Particle identification for the region $|p|$ < 0.7 GeV/c is obtained by dE/dx separation by the vertex detector and the drift chamber

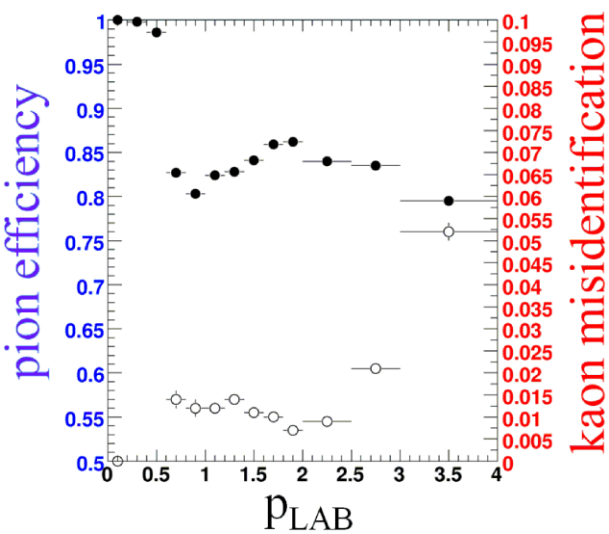

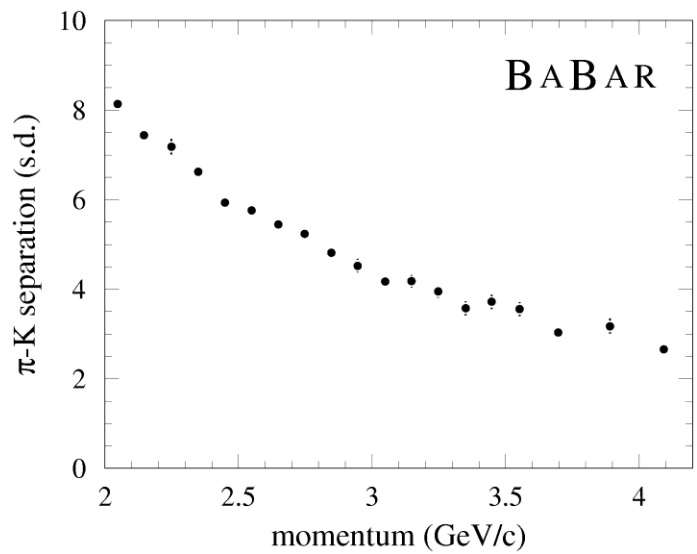

Control sample of D $\rightarrow K^-\pi^+$ events

DIRC

- For $|p|$ > 0.7 GeV/c, particle identification is performed by the DIRC (Detection of Internally Reflected Cherenkov Radiation)

- A charged particle traversing a radiator with refraction index n emits photons on a cone with half opening angle $\cos\theta_c = 1/n\beta$. For n > $\sqrt{2}$ and $\beta \approx 1$, some photons are always totally internally reflected

- Photons are guided down fused silica bars and traverse an expansion region filled with de-ionized water to a PMT array

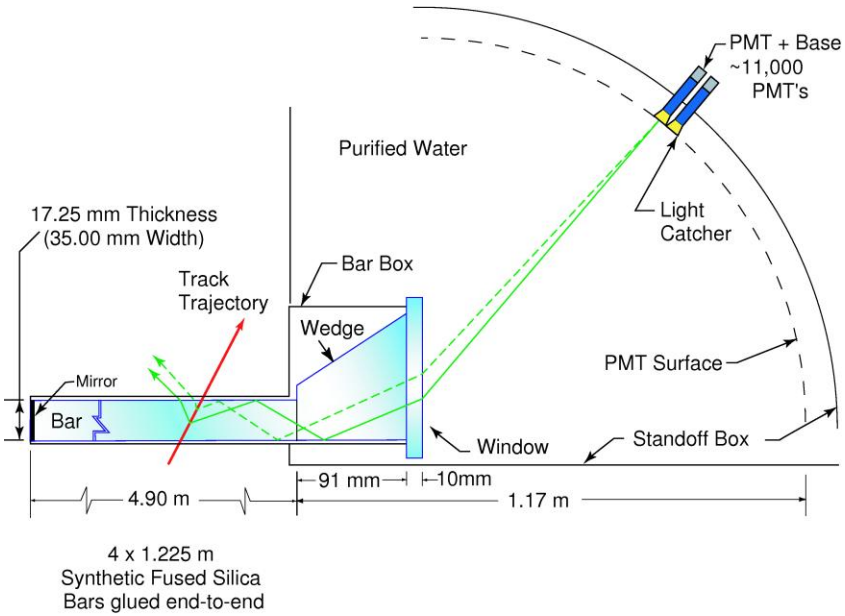

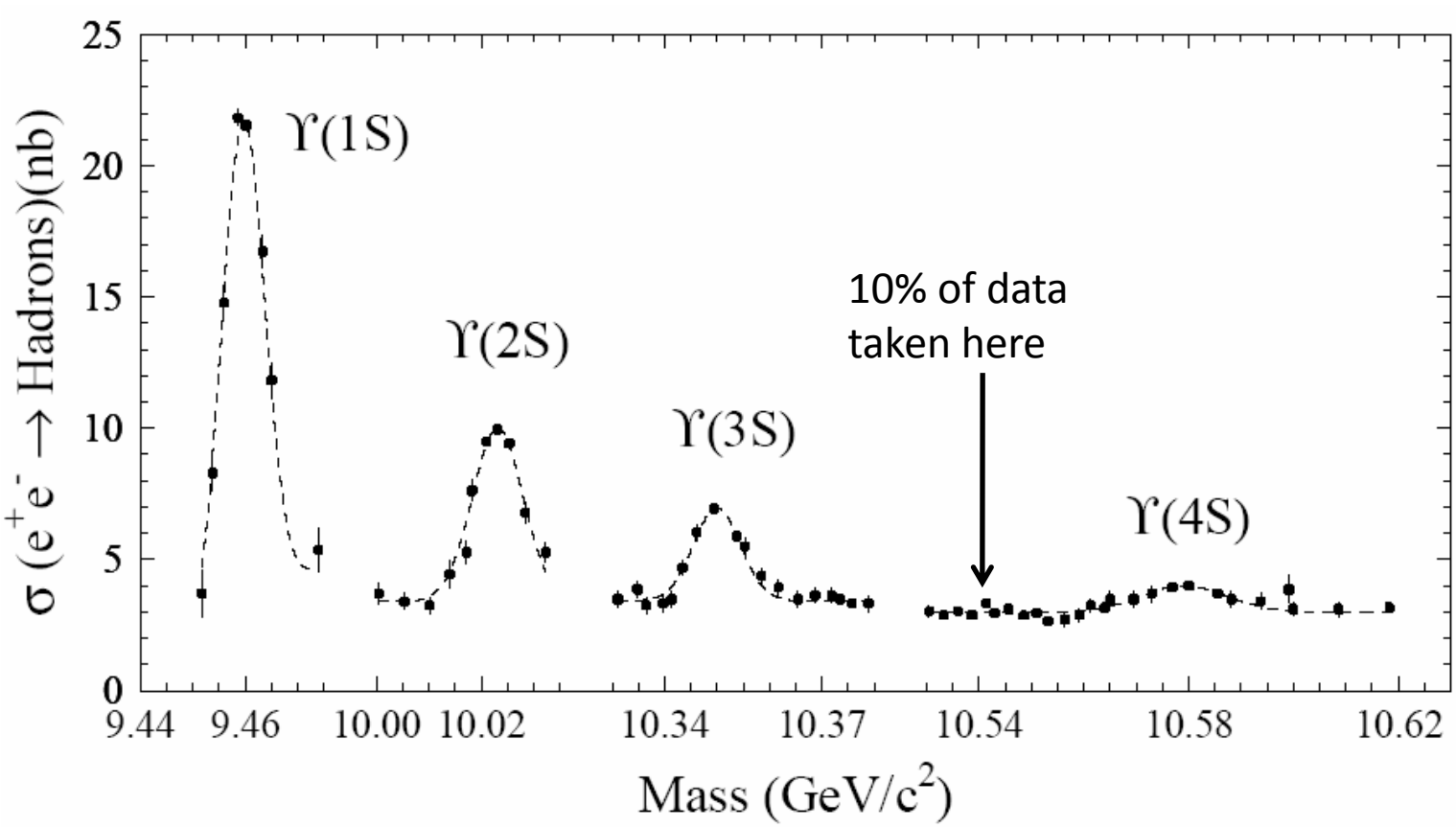

The large majority of data is taken at the $\Upsilon(4S)$. At this energy, the $b\bar{b}$ cross-section is $\approx$ 1.1 nb, while the lighter hadronic cross-section is $\approx$ 3.3 nb.

Measurement of Branching Fractions, CP, and Isospin Asymmetries in $B \to K^*\gamma$

Previous measurements B → K*γ

	PRD 70 (2004) 112006	PRD 69 (2004) 112001
	BABAR $81.9 fb^{-1}$	*Belle* $78.0 fb^{-1}$
$\bar{B}^0 \to K^{*0}\gamma$ $(\times 10^{-5})$	$3.92 \pm 0.20 \pm 0.24$	$4.01 \pm 0.21 \pm 0.17$
$B^+ \to K^{*+}\gamma$ $(\times 10^{-5})$	$3.87 \pm 0.28 \pm 0.26$	$4.25 \pm 0.31 \pm 0.24$
$\mathcal{A}_{CP}$	$-0.013 \pm 0.036 \pm 0.010$	$-0.015 \pm 0.044 \pm 0.012$
Isospin asymmetry	$+0.050 \pm 0.045 \pm 0.028 \pm 0.024$ (measured parameter: Δ_{0-})	$+0.012 \pm 0.044 \pm 0.026$ (measured parameter: Δ_{0+})

Current analysis uses 347 fb^{-1}

Overview

- We reconstruct 4 different modes, which are

$B^0 \rightarrow K^{*0} (K^+\pi^-) \gamma$, $B^0 \rightarrow K^{*0} (K_S\pi^0) \gamma$,
$B^+ \rightarrow K^{*+} (K^+\pi^0) \gamma$, $B^+ \rightarrow K^{*+} (K_S\pi^+) \gamma$.

- We select events using a series of criteria. Some of the major ones are the following:

$1.5 < E^*_\gamma < 3.5$ GeV
Particle Identification
K* mass selection
Veto γ's coming from π^0's and η's

Background suppression

- Major sources of background are continuum (light $q\bar{q}$) events , mis-reconstructed $B \rightarrow X_s\gamma$ and $B \rightarrow K^*\gamma$ events, and $B\bar{B}$ events that decay generically.

- Dominant background is from continuum events, which is suppressed using event topology and angular information.

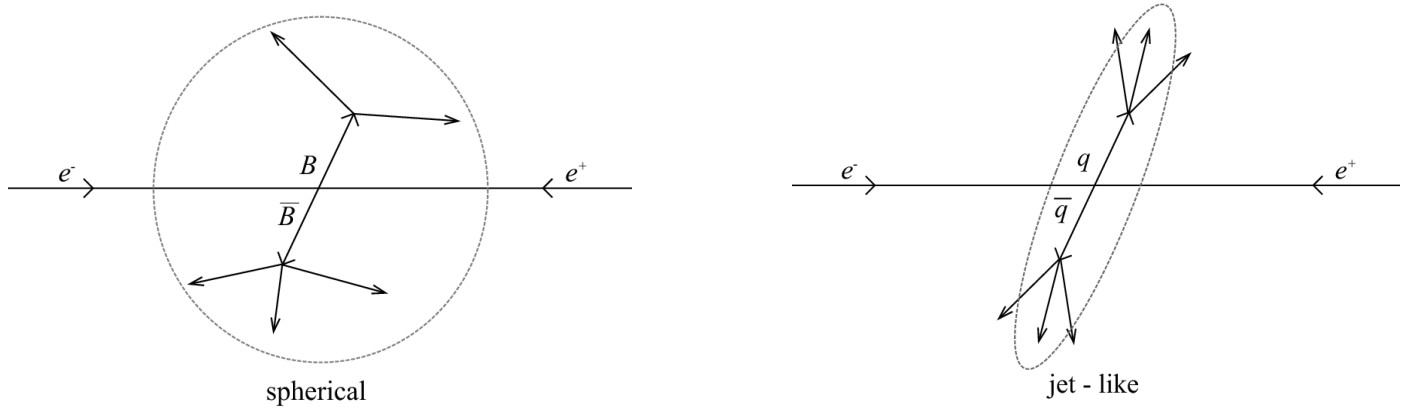

- The background suppression variables are combined into a Neural Network.

Neural Network

- Contains 13 input variables. 9 of these are event shape variables (2nd Fox-Wolfram moment,Legendre moments,..). 4 of these are variables that detect flavor in the rest of the event.

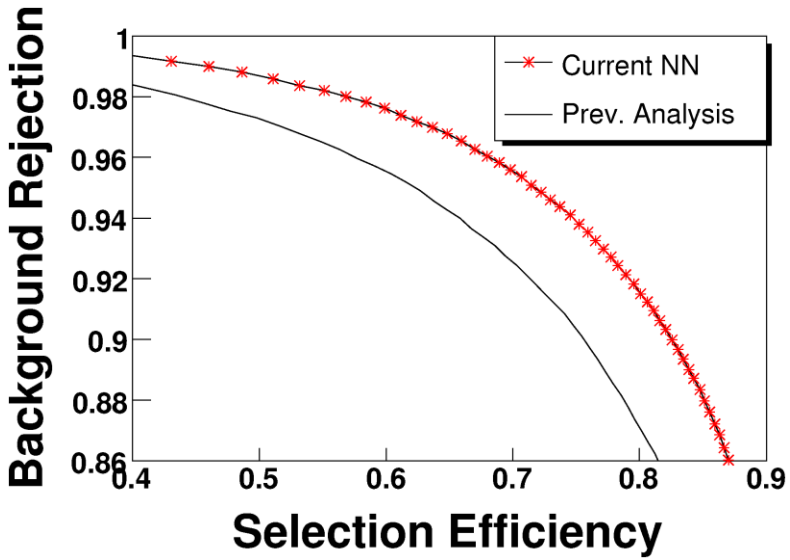

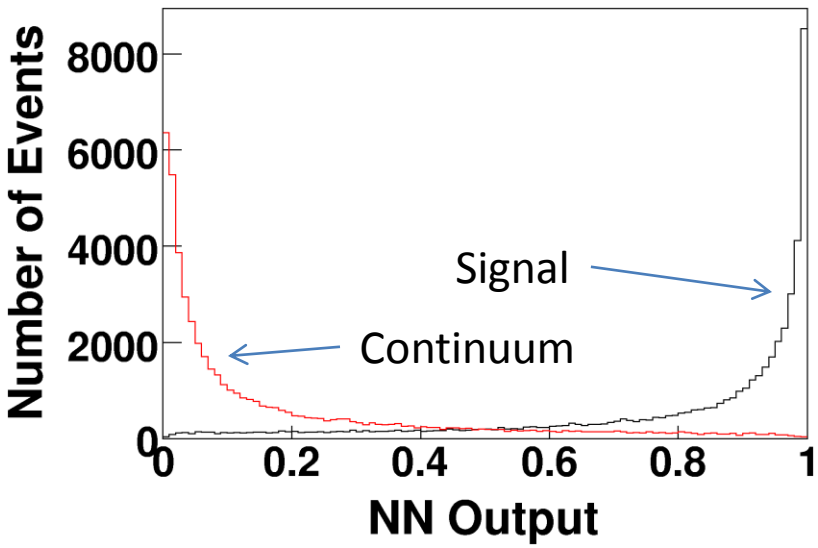

Fit Procedure

- We optimize the selection criteria in the "fit" region, defined as $|\Delta E| < 0.3$ GeV, $m_{ES} > 5.22$, $|\cos\theta_{helicity}| < 0.75$.

1. $m_{ES} = \sqrt{\left(E^{*2}_{beam} - |\vec{p}^{\,*}_{B}|^2\right)}$

2. $\Delta E^{*} = E^{*}_{B} - E^{*}_{beam}$

3. $\cos\theta_{helicity}$ = cosine of angle between the momentum of one of the daughters of the K* and momentum of -B in the K* rest frame

- We use a multidimensional maximum likelihood fit with different components for signal and background ($q\bar{q}$, $B\bar{B}$). There are 3 dimensions (m_{ES}, ΔE, $\cos\theta_{helicity}$) and 3 components (signal, $B\bar{B}$, $q\bar{q}$).

m_{ES} fit projections

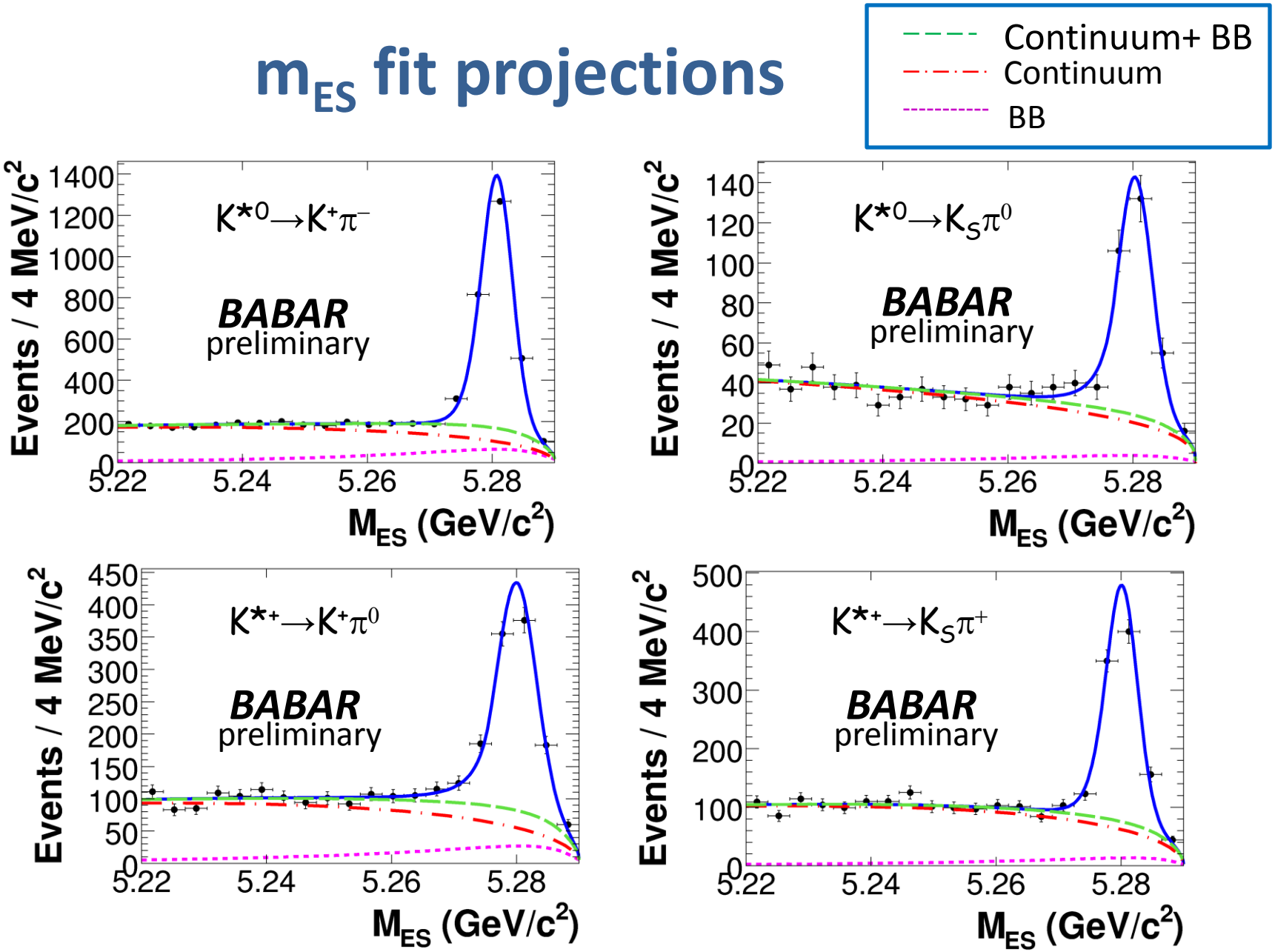

ΔE fit projections

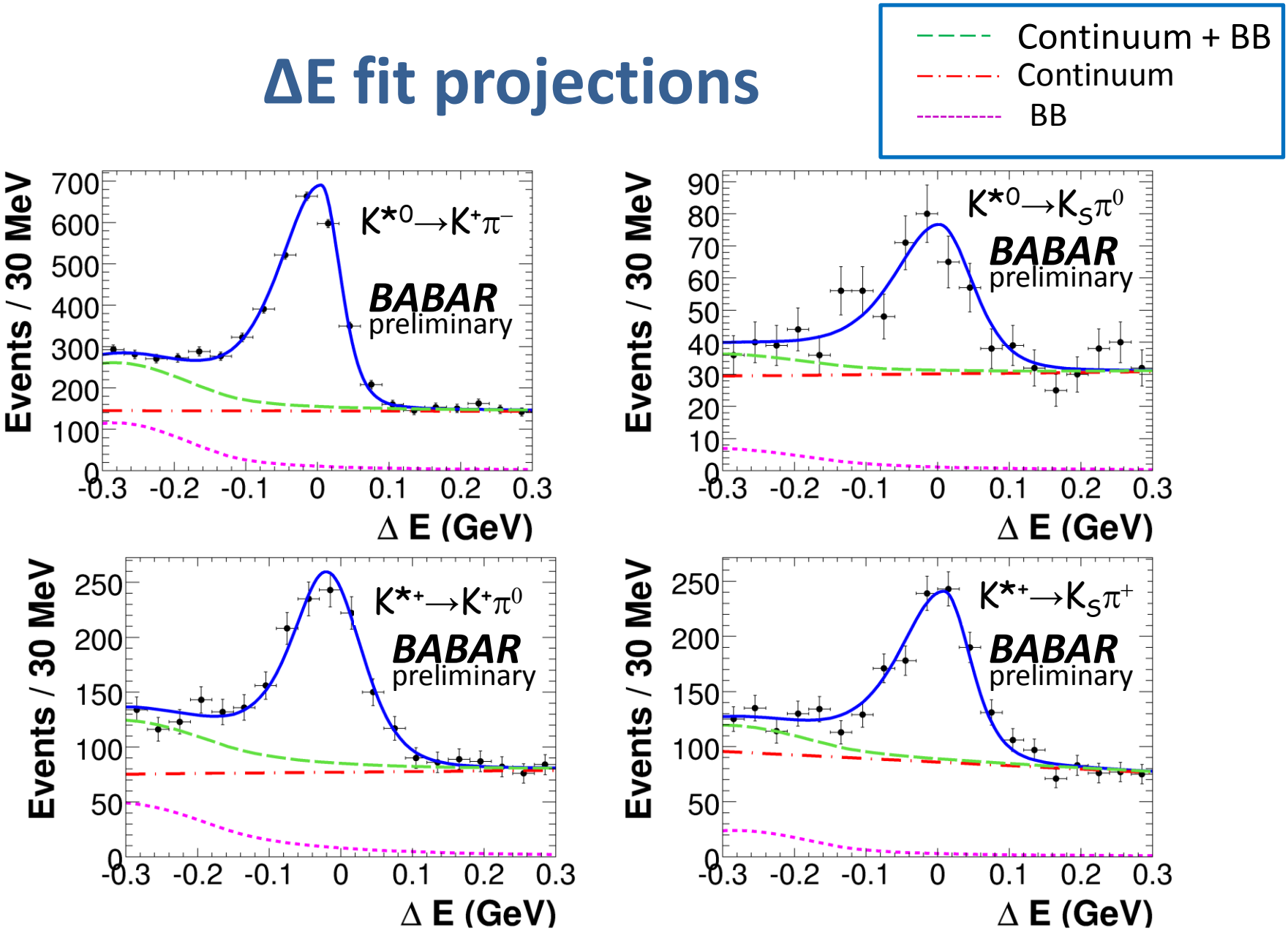

Branching Fraction and Isospin Asymmetry Results

Mode	$\epsilon(\%)$	N_S	$\mathcal{B}(\times 10^{-5})$	Combined $\mathcal{B}(\times 10^{-5})$
$K^+\pi^-$	21.8 ± 0.8	2400.0 ± 55.4	$4.45 \pm 0.10 \pm 0.17$	$4.47 \pm 0.10 \pm 0.16$
$K_s\pi^0$	13.0 ± 0.9	256.0 ± 20.6	$4.66 \pm 0.37 \pm 0.35$	
$K^+\pi^0$	15.3 ± 0.8	872.7 ± 37.6	$4.38 \pm 0.19 \pm 0.26$	$4.22 \pm 0.14 \pm 0.16$
$K_s\pi^+$	20.1 ± 0.7	759.1 ± 33.8	$4.13 \pm 0.18 \pm 0.16$	

The isospin asymmetry is $\Delta_{0-} = 0.066 \pm 0.021$ (stat.) $\pm$ 0.022(sys.), and the 90% confidence interval for Δ_{0-} is $0.017 < \Delta_{0-} < 0.116$.

CP Asymmetry

- We use the modes $B^0 \to K^{*0} (K^+\pi^-)\ \gamma$, $B^+ \to K^{*+} (K^+\pi^0)\ \gamma$, $B^+ \to K^{*+} (K_S\pi^+)\ \gamma$.

- The fit is identical to the one used for the branching fractions. However, now we fit for the 3 CP asymmetry parameters of the 3 components ($a_{CP,Sig}$, $a_{CP,\ B\ Bkg}$, $a_{CP,\ Cont\ Bkg}$).

Mode	$\mathcal{A}$	Combined $\mathcal{A}$
$K^+\pi^-$	$-0.016 \pm 0.022 \pm 0.007$	$-0.003 \pm 0.017 \pm 0.007$
$K_s\pi^0$		
$K^+\pi^0$	$+0.040 \pm 0.039 \pm 0.007$	
$K_s\pi^+$	$-0.006 \pm 0.041 \pm 0.007$	

Experimental Status

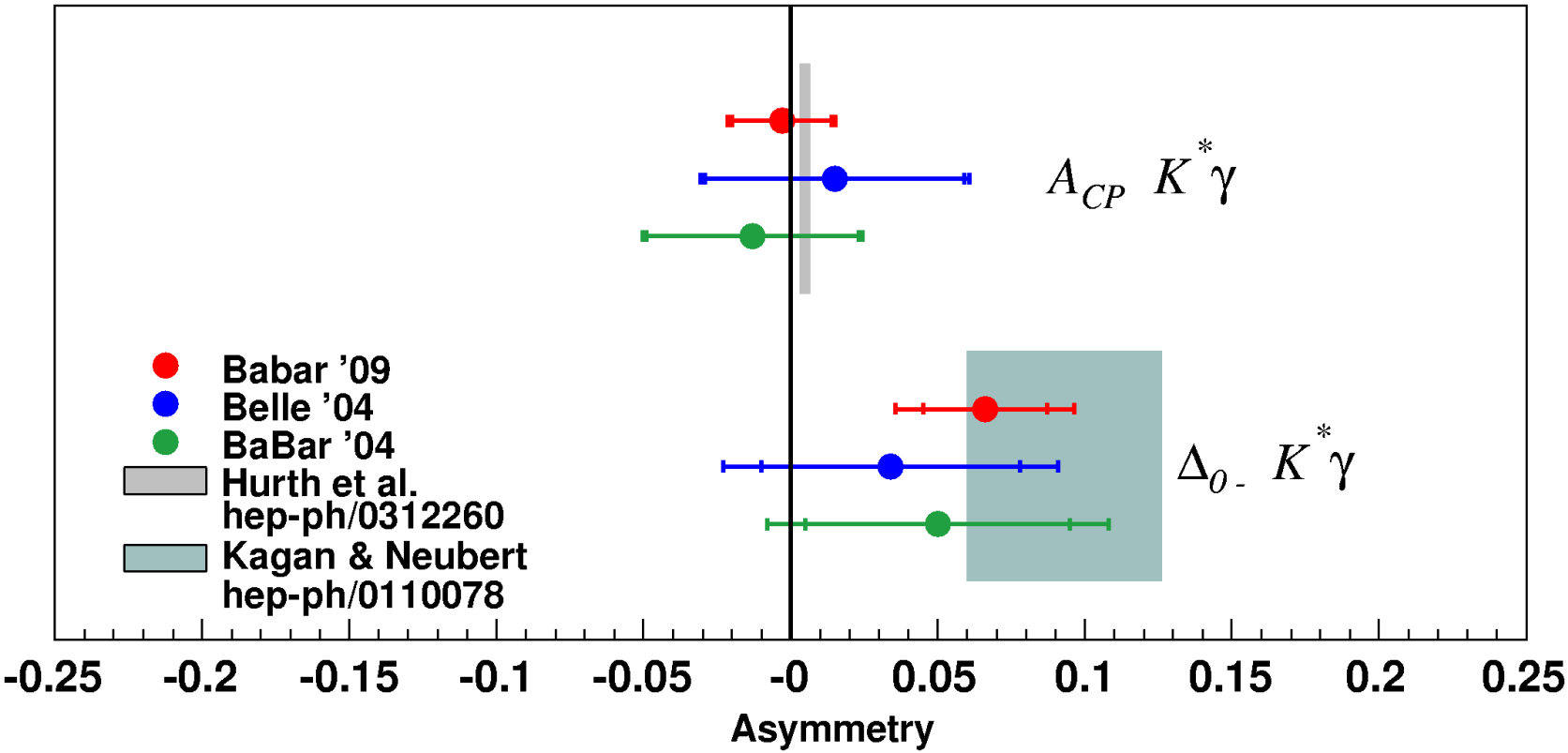

Measurement of $B \to \rho(\omega)\gamma$ decays

Previous measurements of B → ρ(ω)γ

	PRL 84 (2000)5283	PRL 94 (2005) 011801	PRL 96 (2006) 221601
	CLEOII $9.2 fb^{-1}$	*BABAR* $191 fb^{-1}$	*Belle* $350.9 fb^{-1}$
$B^+ \to \rho^+\gamma(\times 10^{-6})$	< 13	< 1.8	$0.55^{+0.42+0.36}_{-0.36-0.08}$ (1.6σ)
$B^0 \to \rho^0\gamma(\times 10^{-6})$	< 17	< 0.4	$1.25^{+0.37+0.07}_{-0.33-0.06}$ (5.2σ)
$B^0 \to \omega\gamma(\times 10^{-6})$	< 92	< 1.0	$0.56^{+0.34+0.05}_{-0.27-0.10}$ (2.3σ)
$B \to (\rho/\omega)\gamma(\times 10^{-6})$		< 1.2	$1.32^{+0.34+0.10}_{-0.31-0.09}$ (5.1σ)

Overview

- We reconstruct 3 different modes:

$B^0 \to \rho^0 (\pi^+\pi^-) \gamma$, $B^0 \to \omega (\pi^+\pi^-\pi^0) \gamma$,
$B^+ \to \rho^+ (\pi^+\pi^0) \gamma$

- We select events using criteria similar to the K* analysis. Dominant background is still continuum. However, the K* background also plays a prominent role, as the BR($B \to K^*\gamma$) ≈ 40 times higher.

- We use a neural network to distinguish between continuum and signal events, and perform an unbinned maximum likelihood fit.

Neural Network

- The neural network contains 33 input variables. It is the same as the K* analysis, with the addition of variables that pertain to the kinematic properties of the e, μ, K in the rest of the event (18).

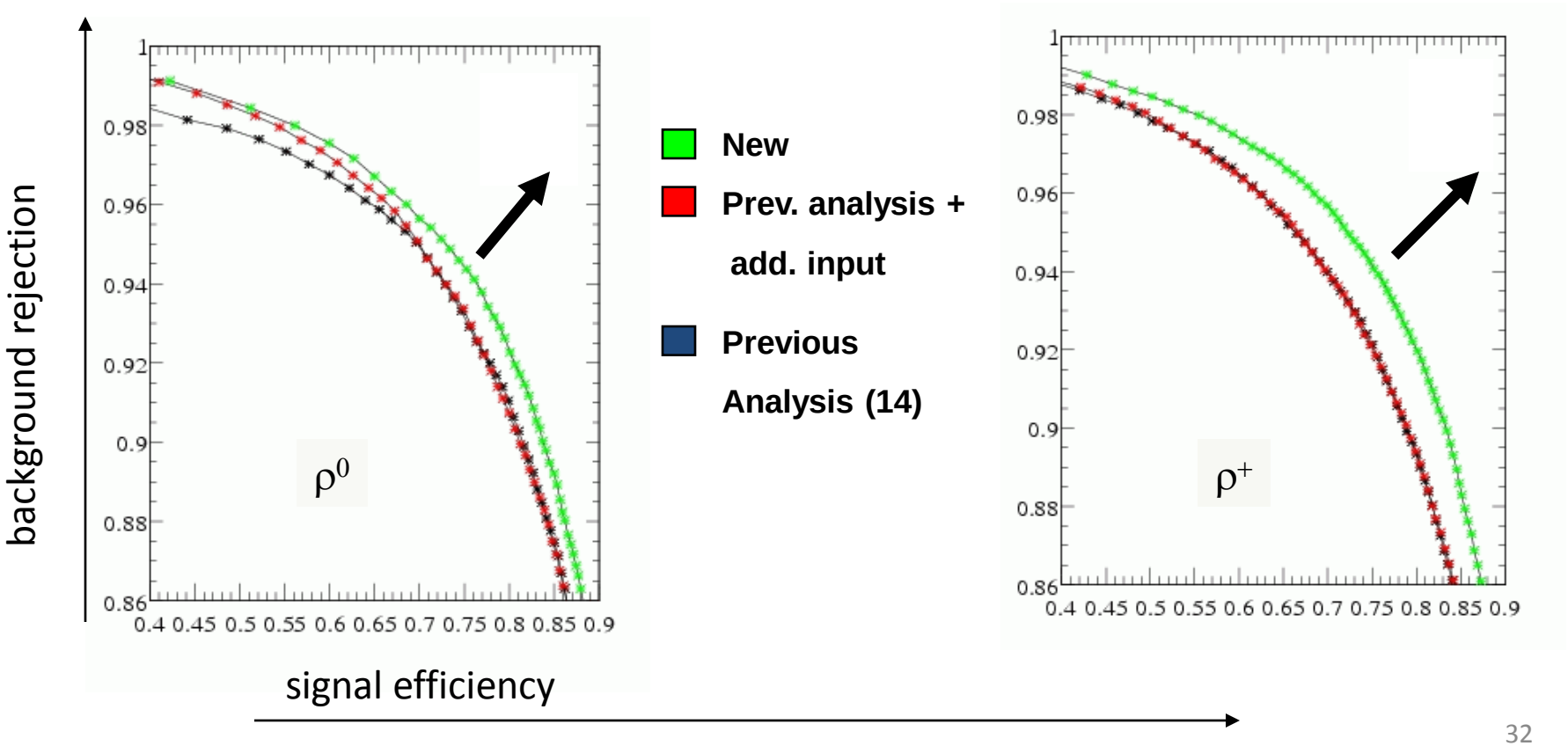

Fit Procedure

- We perform an unbinned maximum likelihood fit. There are 4 dimensions for $\rho\gamma$ and 5 for $\omega\gamma$.

- The fit variables are m_{ES}, ΔE^*, transformed NN output, $\cos\theta_{helicity}$ + $\cos\theta_{dalitz}$ ($\omega\gamma$).

$\theta_{helicity}(\rho\gamma)$ = angle between π^+ and B in ρ rest frame
$\theta_{helicity}(\omega\gamma)$ = angle between the normal of $\pi^+\pi^-$ plane and B in ω rest frame
$\theta_{dalitz}(\omega\gamma)$ = angle between π^0 and π^+ in $\pi^+\pi^-$ rest frame

transformed NN output $= \tanh^{-1}\left(\frac{(NN - c_1)\cdot(1 - c_2)}{c_3}\right), \quad c_i = \text{constant}$

- The $\rho^0\gamma$ fit has $K^{*0}\gamma$ and $K^{*+}\gamma$ as separate components, while the $\rho^+\gamma$ fit treats $K^{*+}\gamma$ ($K^{*+}\rightarrow K^+\pi^0$) separately

$B^+ \rightarrow \rho^+\gamma$ fit projections

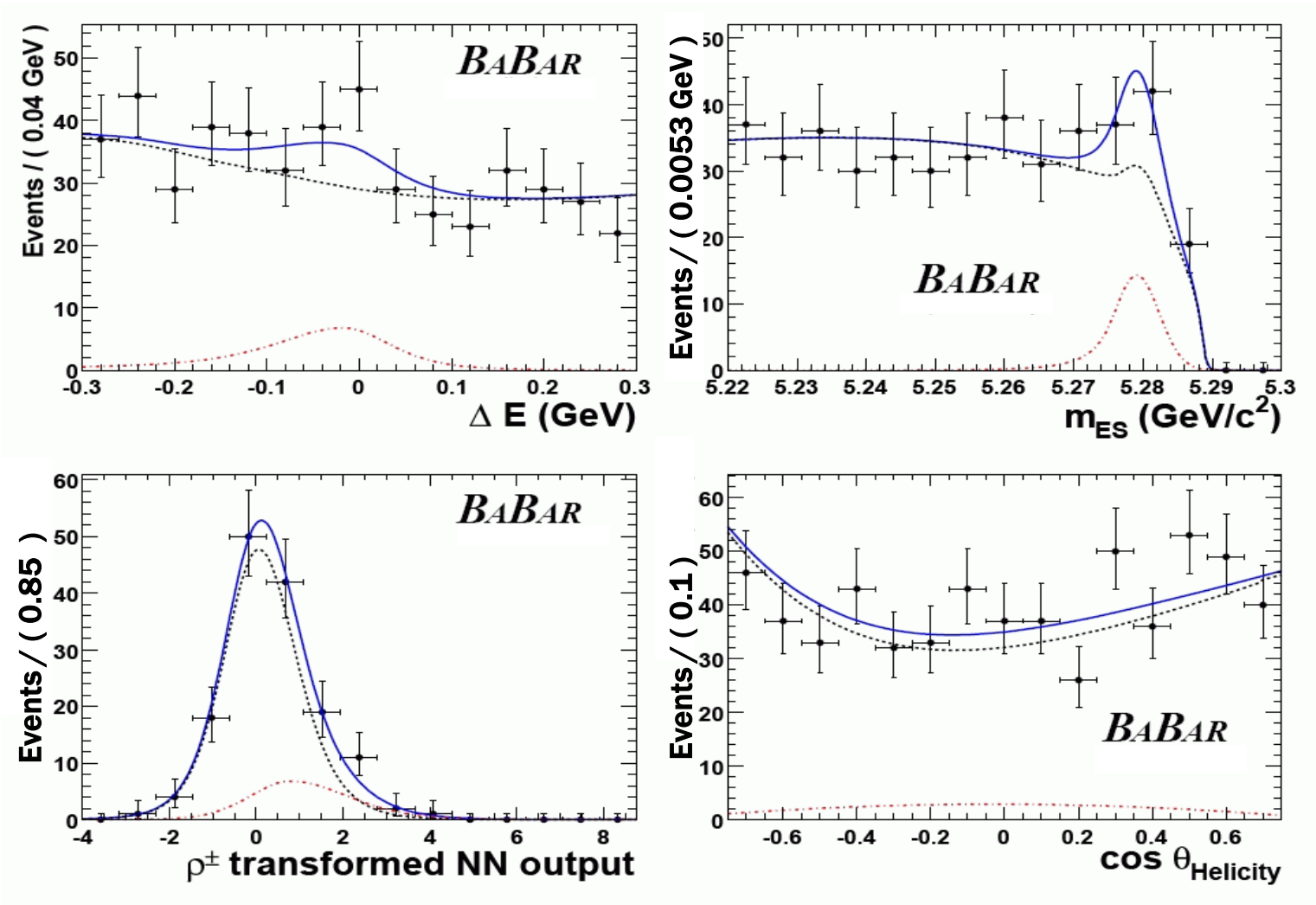

$B^0 \to \rho^0 \gamma$ fit projections

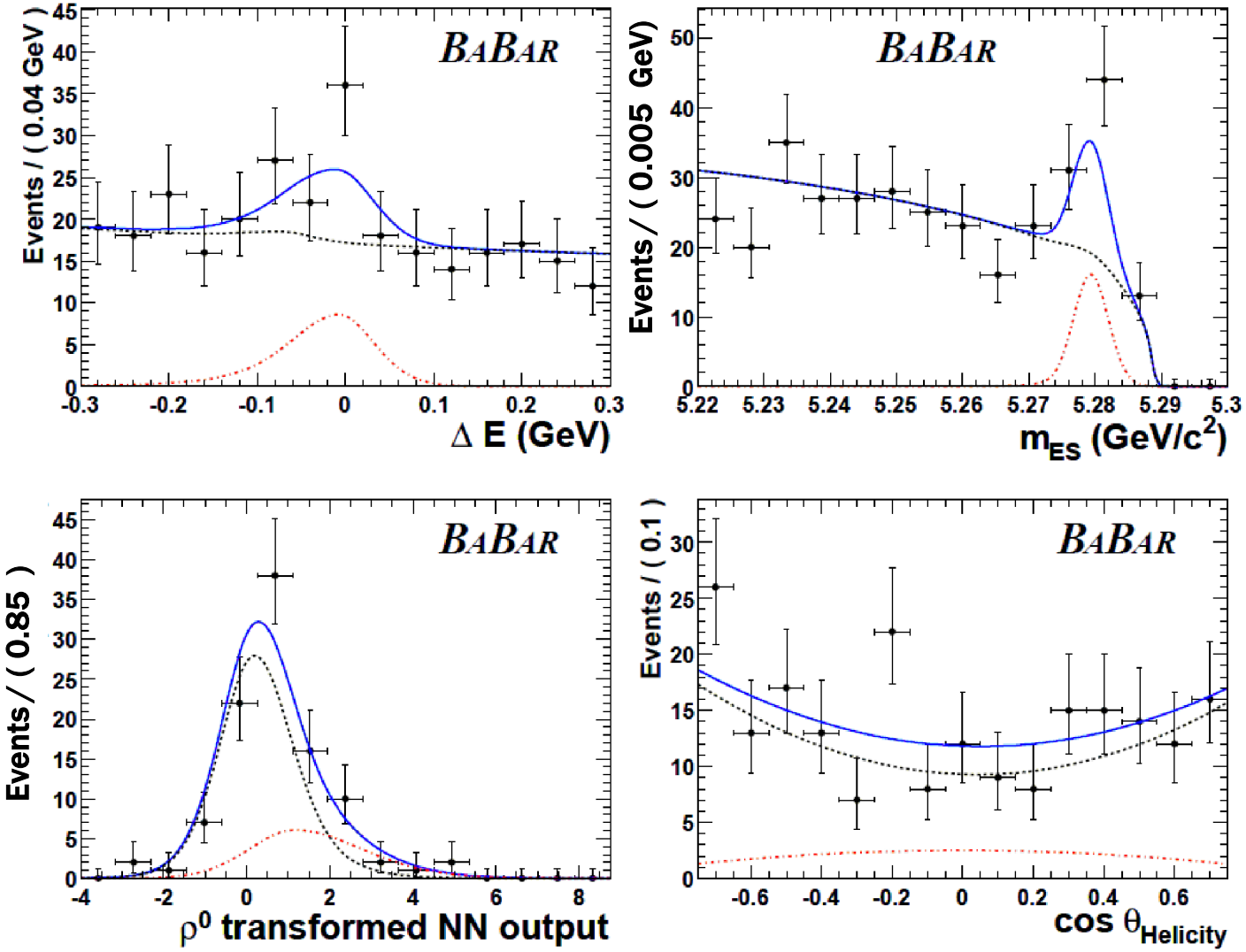

Results

Mode	$n_{\rm sig}$	Σ	$\epsilon(\%)$	$\mathcal{B}(10^{-6})$
$B^+ \to \rho^+\gamma$	$42.0^{+14.0}_{-12.7}$	3.8σ	11.0	$1.10^{+0.37}_{-0.33} \pm 0.09$
$B^0 \to \rho^0\gamma$	$38.7^{+10.6}_{-9.8}$	4.9σ	14.1	$0.79^{+0.22}_{-0.20} \pm 0.06$
$B^0 \to \omega\gamma$	$11.0^{+6.7}_{-5.6}$	2.2σ	7.9	$0.40^{+0.24}_{-0.20} \pm 0.05$
$B \to (\rho/\omega)\gamma$		6.4σ		$1.25^{+0.25}_{-0.24} \pm 0.09$
$B \to \rho\gamma$		6.0σ		$1.36^{+0.29}_{-0.27} \pm 0.10$

Isospin asymmetry:

$$\frac{\Gamma(B^+ \to \rho^+\gamma)}{2\Gamma(B^0 \to \rho^0\gamma)} - 1 = -0.35 \pm 0.27$$

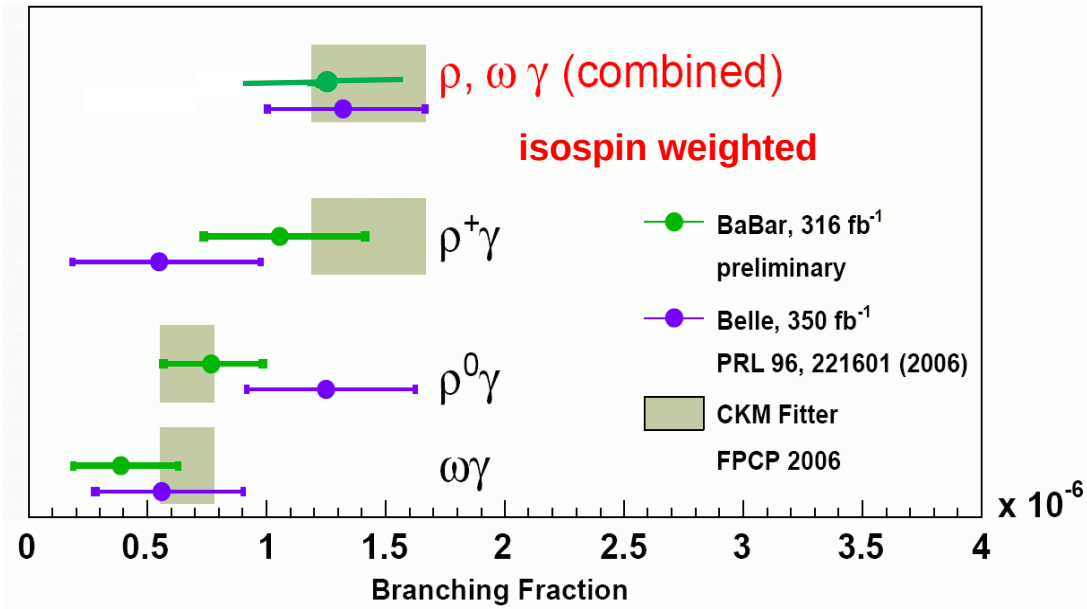

$\left|\frac{V_{td}}{V_{ts}}\right|$ comparisons

$$\left|\frac{V_{td}}{V_{ts}}\right| = 0.200\ ^{+0.021}_{-0.020}\,(\text{exp})\ \pm 0.015\ (\text{theory})$$

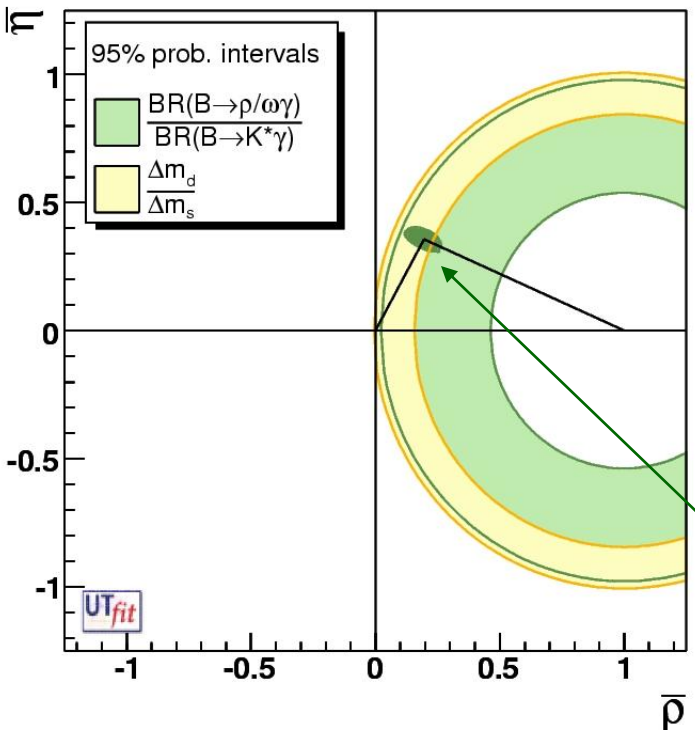

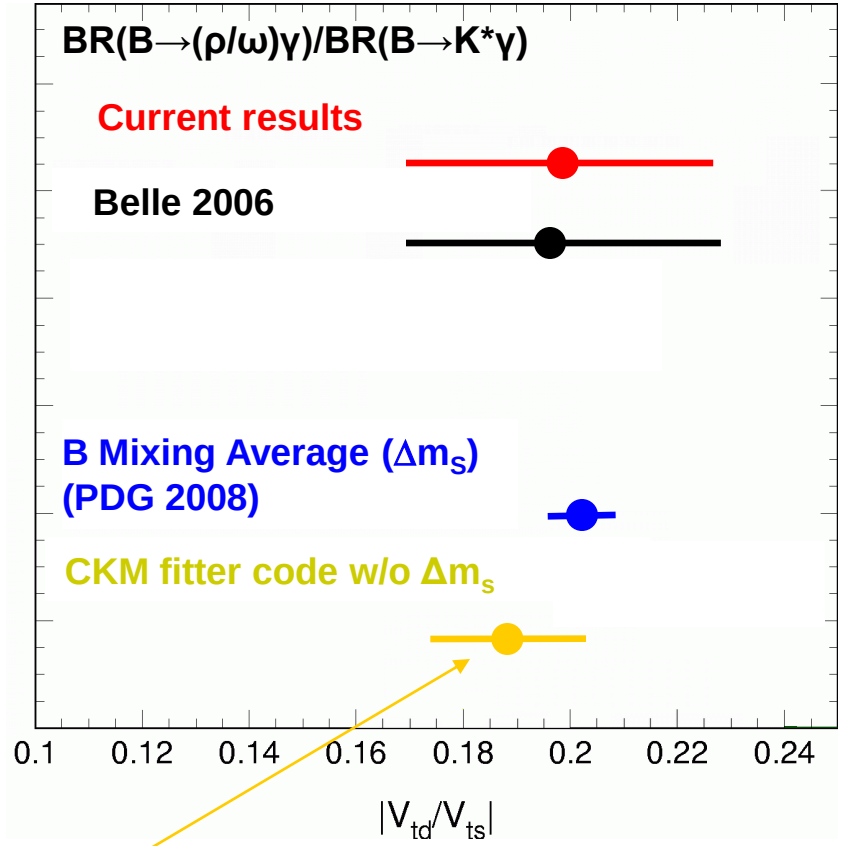

Global fit excludes Δm_s and $B\to\rho(\omega)\gamma$

Search for $B \to \varphi\gamma$

Standard Model Diagram

- The dominant diagram for B $\rightarrow \varphi\gamma$ is

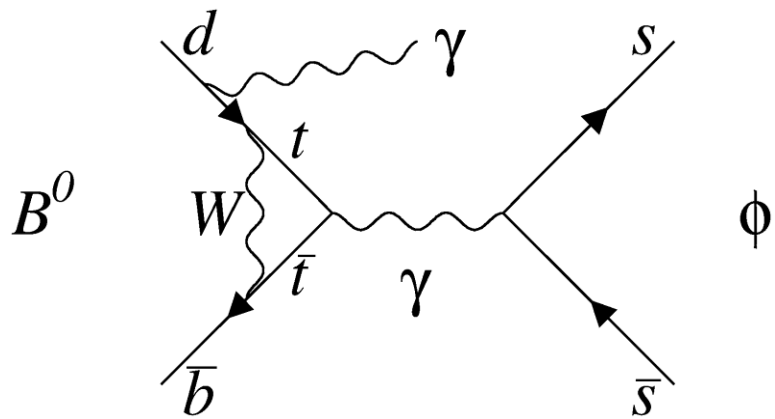

- The suppression is given by $G_F^2\alpha_{EM}^3$. The Standard Model predictions are $\approx 10^{-12}$.

Overview

- CLEO has yielded BF($B \rightarrow \varphi\gamma$) < 3.3×10^{-6} (PRL 84 (2000) 5283)

- We follow the same procedure as the previously described analyses. In particular, we apply a neural network for continuum discrimination. However, the BB background is negligible due to the small width of the φ.

- The background is determined by fitting in the sideband regions and extrapolating into the signal region.

Results

- 8 events in the signal box. Upper limit at the 90% confidence level on the number of signal events is 7.99.

- Upper limit at the 90% confidence level on the branching fractions is

$$\mathrm{BF} = \frac{\mathrm{N}^{90}{}_{\mathrm{UL}}}{\varepsilon_s \times 2 \times N_{B^0\overline{B}^0} \times \mathrm{BF}(\phi \to \mathrm{K}^+\mathrm{K}^-)}(1+1.15\sigma^2{}_r)$$

where ε_s= (13.9 0.1 (stat) 0.7 (sys.))%. The upper limit on the branching fraction is 9.4 x 10^{-7}

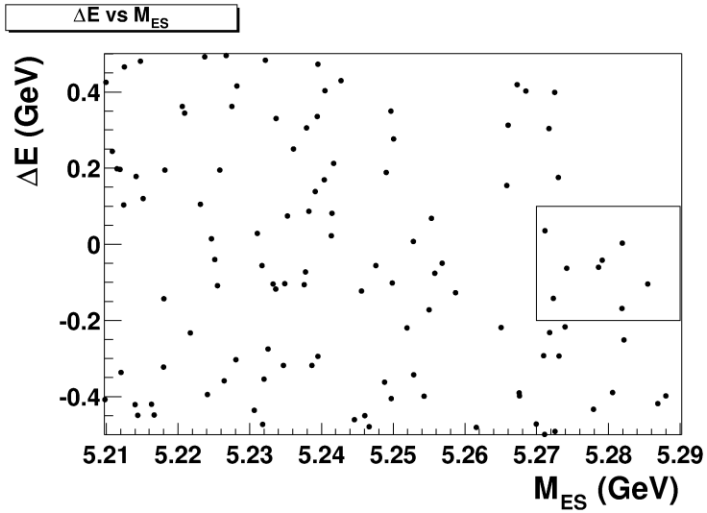

Conclusions

- Most precise measurements of branching fractions, CP, and isospin asymmetries of $B \to K^*\gamma$ (under PRL review) (arXiv:0906.2177)
- Observed the decay $B^0 \to \rho^0\gamma$ now , and found the first evidence for the decay $B^+ \to \rho^+\gamma$. The combined branching fraction from Babar is

$$\mathrm{BF}[\mathrm{B} \to (\rho,\omega)\gamma] = (1.25^{+0.25}_{-0.24} \pm 0.09) \times 10^{-6}$$

This is used to obtain

$$\left|\frac{V_{td}}{V_{ts}}\right| = 0.200^{+0.021}_{-0.020}\,(\mathrm{exp}) \pm 0.015\,(\mathrm{theory})$$

(PRL 98 151802(2007))

- Set the most stringent upper limit on $\mathrm{BF}(B \to \varphi\gamma)$ (PRD 72 091103(2005))

Backup Slides

Another method to extract $|V_{td}/V_{ts}|$ is to use B mixing. The dominant diagram is

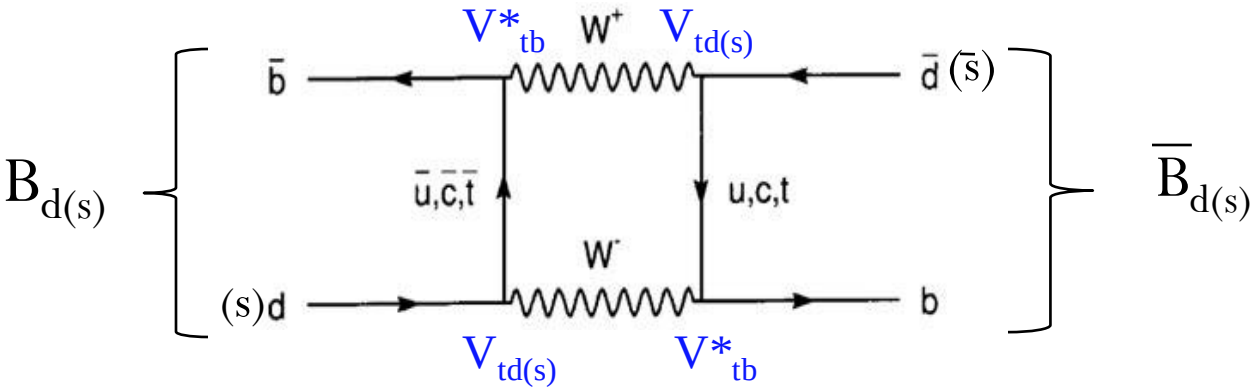

This method gives the value of

$$|V_{td}/V_{ts}| = 0.207 \pm 0.001_{exp} \pm 0.006_{theo} \text{ (PDG 2008).}$$

How do penguins fit in the picture? The Standard Model effects are suppressed relative to mixing, and the measurement of $|V_{td}/V_{ts}|$ could show deviations from B mixing. The mixing parameter x_d is

$$x_d = \Delta m_B/\Gamma_B \approx 1 \Rightarrow \Delta m_B \approx \Gamma_B$$

while

$$Br(B \to \rho\gamma) \approx 10^{-6} \Rightarrow \Gamma_{\rho\gamma} \approx 10^{-6}\,\Gamma_B$$

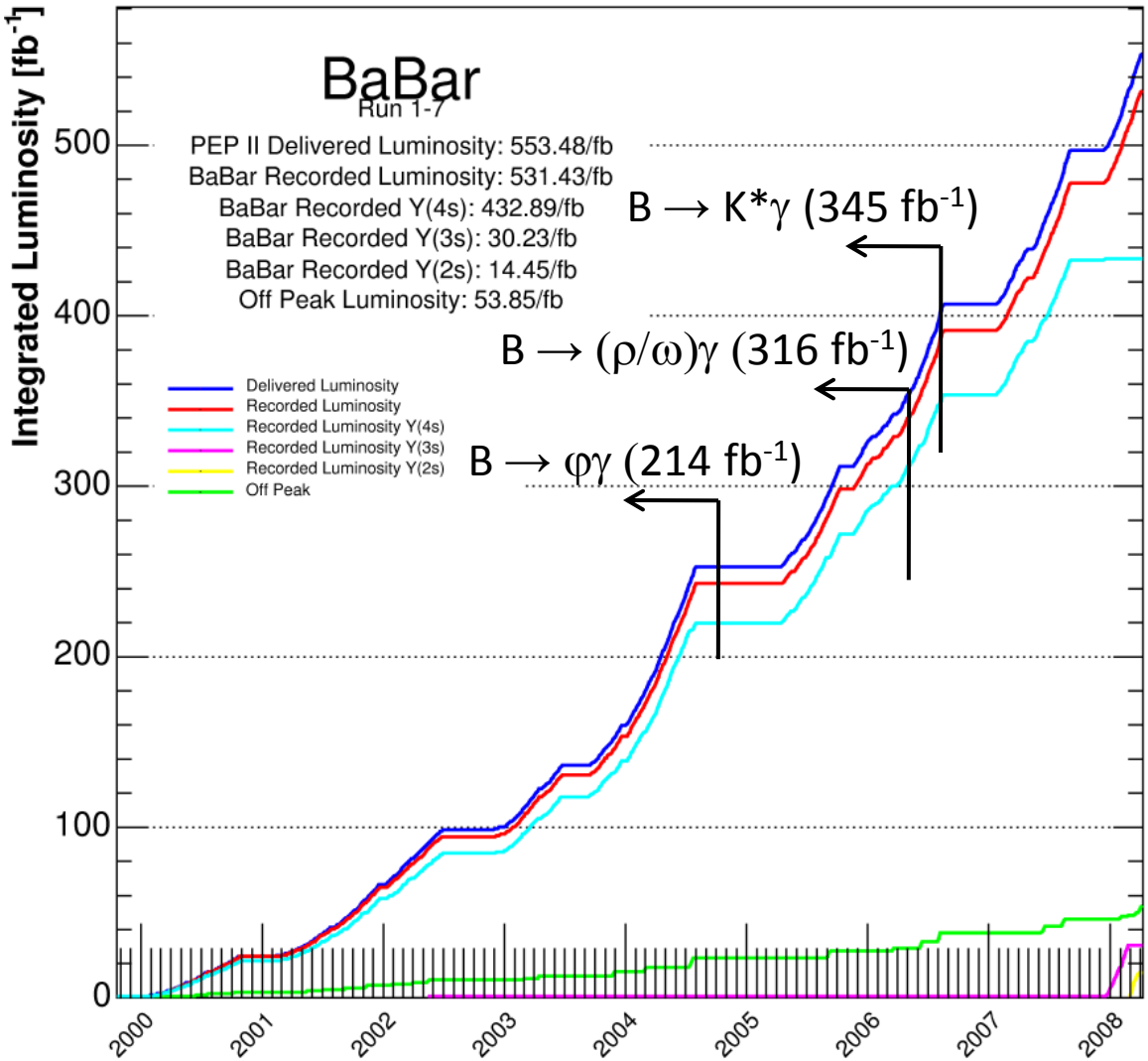
BaBar
Run 1-7
PEP II Delivered Luminosity: 553.48/fb
BaBar Recorded Luminosity: 531.43/fb
BaBar Recorded Y(4s): 432.89/fb
BaBar Recorded Y(3s): 30.23/fb
BaBar Recorded Y(2s): 14.45/fb
Off Peak Luminosity: 53.85/fb
Delivered Luminosity
Recorded Luminosity
Recorded Luminosity Y(4s)
Recorded Luminosity Y(3s)
Recorded Luminosity Y(2s)
Off Peak
B → K*γ (345 fb-1)
B → (ρ/ω)γ (316 fb-1)
B → φγ (214 fb-1)
Integrated Luminosity [fb-1]
0
100
200
300
400
500
2000
2001
2002
2003
2004
2005
2006
2007
2008

We select signal Monte Carlo events and generate the background events from the background PDFs. We perform an independent series of fits. Here,

$$\text{Pull} = \frac{\text{(\# of fitted events) – (\# of generated events)}}{\text{error of signal yield}}$$

	$B^0 \to K^{*0}\gamma$		$B^+ \to K^{*+}\gamma$	
	$K^{*0} \to K^+\pi^-$	$K^{*0} \to K_S\pi^0$	$K^{*+} \to K^+\pi^0$	$K^{*+} \to K_S\pi^+$
Nominal Pull				
Sig. Pull	-0.814±0.12	-0.630±0.062	-0.751±0.15	-0.697±0.12
Cont. Pull	0.56±0.11	0.092±0.058	0.12±0.12	0.24±0.11
$B\overline{B}$	-0.076±0.098	0.206±0.061	0.22±0.13	-0.10±0.10

Some bias is noticed. This is taken into account by correcting the signal efficiency.

Here is the composition of the $B\overline{B}$ background per mode.

$B \to K^*\gamma$ mode	$B\overline{B}$ backgrounds (% of total $B\overline{B}$ background)
$B^0 \to K^{*0}\gamma, K^{*0} \to K^+\pi^-$	$B \to X_s\gamma$ (81%) $B^0 \to K^{*0}\eta, K^{*0} \to K^+\pi^-$ (5%) $B^+ \to K^{*+}\gamma, K^{*+} \to K^+\pi^0$ (5%)
$B^0 \to K^{*0}\gamma, K^{*0} \to K_S\pi^0$	$B \to X_s\gamma$ (75%) $B^+ \to K^{*+}\gamma, K^{*+} \to K_S\pi^+$ (11%)
$B^+ \to K^{*+}\gamma, K^{*+} \to K^+\pi^0$	$B \to X_s\gamma$ (72%) $B^+ \to K^{*+}\eta, K^{*+} \to K^+\pi^0$ (4%) $B^0 \to K^{*0}\gamma, K^{*0} \to K^+\pi^-$ (11%)
$B^+ \to K^{*+}\gamma, K^{*+} \to K_S\pi^+$	$B \to X_s\gamma$ (79%) $B^+ \to K^{*+}\eta, K^{*+} \to K_S\pi^+$ (6%) $B^0 \to K^{*0}\gamma, K^{*0} \to K_S\pi^0$ (8%)

Now, we select $B\overline{B}$ background Monte Carlo events from the previous slide, while the other two components are from the PDFs. An series of independent fits is again performed.

	$B^0 \to K^{*0}\gamma$		$B^+ \to K^{*+}\gamma$	
	$K^{*0} \to K^+\pi^-$	$K^{*0} \to K_S\pi^0$	$K^{*+} \to K^+\pi^0$	$K^{*+} \to K_S\pi^+$
Nominal Pull				
Sig. Pull	-0.136±0.16	0.27±0.17	0.15±0.15	0.17±0.18
Cont. Pull	0.020±0.14	0.40±0.14	0.46±0.13	0.36±0.17
$B\overline{B}$	-0.107±0.15	-0.807±0.14	-0.824±0.14	-0.570±0.16

This time, there are no significant biases.

Here are the comparison of the fit results to K* mass to the PDG values.

	Data		PDG Value	
Mode	m (MeV)	Γ(MeV)	m (MeV)	Γ(MeV)
$K^{*0} \to K^+\pi^-$	894.47± .68	49.1± 1.6	896.00± .25	50.3± 0.6
$K^{*0} \to K_S\pi^0$	893.6± 1.6	37.8± 3.6	896.00± .25	50.3± 0.6
$K^{*+} \to K^+\pi^0$	891.3± 1.2	50.5± 2.6	891.66± .26	50.8± 0.9
$K^{*+} \to K_S\pi^+$	894.2± 1.1	43.5± 2.4	891.66± .26	50.8± 0.9

We now turn to validating the fit model. This is done by performing studies in which we select Monte Carlo events for a particular component, while the other components have events generated from the probability distribution function (PDF). We then fit for these events, in which a series of fits is performed. This procedure is performed to understand any biases the fit model may have.

The K* resonance is modeled as a relativistic P-wave Breit-Wigner.

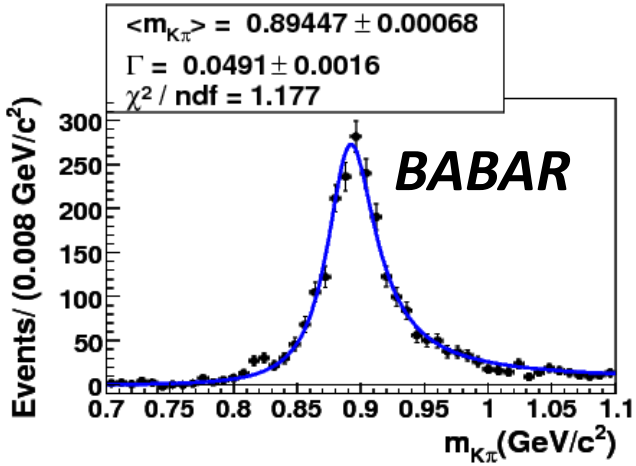

$K^{*0} \to K^+\pi^-$ mode

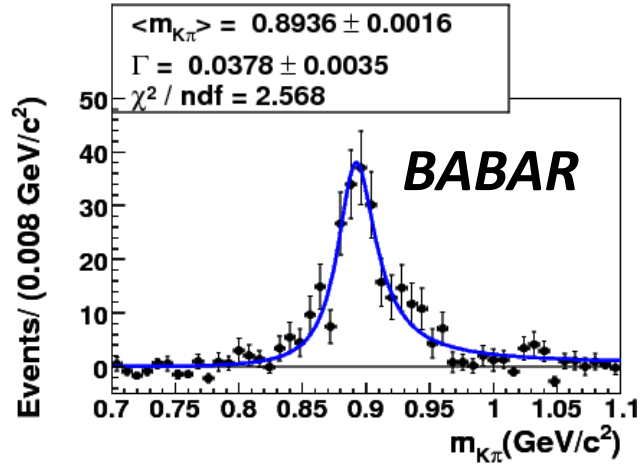

$K^{*0} \to K_S\pi^0$ mode

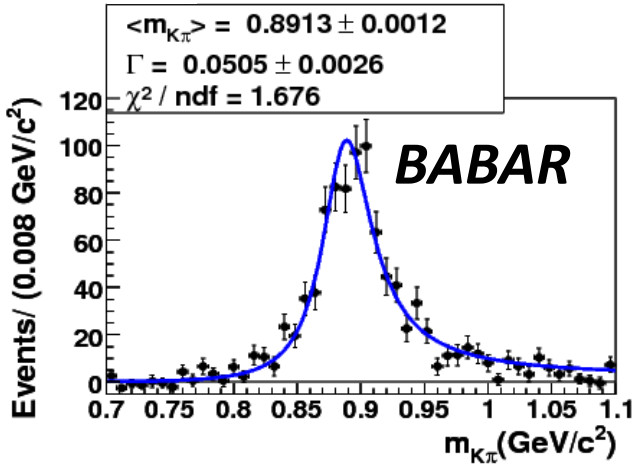

$K^{*+} \to K^+\pi^0$ mode

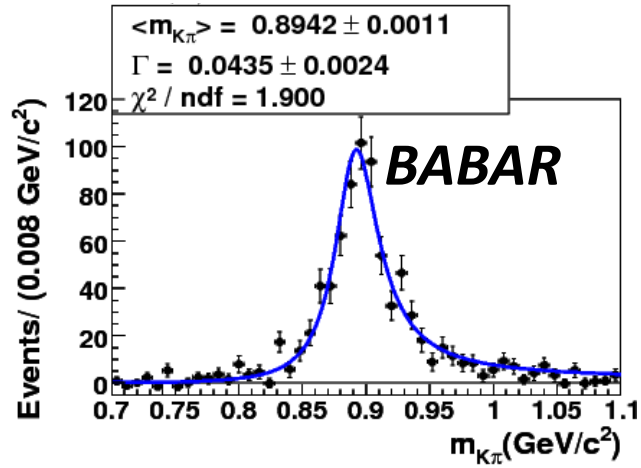

$K^{*+} \to K_S\pi^+$ mode